Proceedings of 10th International Conference on Precision, Meso, Micro and Nano Engineering (COPEN 10)
December 07 – 09, 2017, Indian Institute of Technology Madras, Chennai – 600 036 INDIA

Finite Element Method Based Numerical Simulation of Laser Beam Welded Titanium Alloy (Ti-6Al-4V)

Chandan Kumar, Manas Das*,

Department of Mechanical Engineering
Indian Institute of Technology, Guwahati - 781039, Assam, INDIA

Abstract

In the present study a FEM based numerical simulation of transient temperature profile of laser beam welding process is described in detail. A 3-D finite element modeling is employed for this purpose using FEM package of ANSYS® 14. A 3-D conical Gaussian heat source model, moving with constant speed is considered for performing transient thermal analysis. The temperature dependent material properties of Ti-6Al-4V alloy are considered including convective and radiative boundary conditions. The effect of laser beam power and welding speed on the transient temperature profile, weld bead features, and the size of heat affected zone are investigated. It is observed that peak temperature in the fusion zone is directly proportional to the welding power and inversely proportional to the welding speed. The shape of weld pool, bead width and its depth of penetration depend on the welding power and traverse speed of laser heat source. It is also noticed that size of the heat affected zone is strongly affected by the welding power and traverse speed. The present model helps to optimize the laser beam welding process. It also provides a consistent estimation of the temperature field at different locations of the welded specimen and helps in reducing the cost of experiments.

Keywords: Laser beam welding, Ti-6Al-4V alloy, FEM, Thermal analysis, Gaussian heat source.

1. INTRODUCTION

Titanium and its alloys serve as a bridge between the ideal properties of aluminium and steel. Ti-6Al-4V (Ti64) alloy is supreme combination of strength and ductility. Therefore, it is widely used in many areas such as automotive, aerospace, nuclear, chemical, and medical industries, etc. It possesses light weight, better corrosion resistance, and excellent biocompatibility [1, 2]. Welding is the most versatile joining process which is applicable for the fabrication of several products used in many industries. Different types of energy sources are commonly used for welding such as gas flame, electric arc, laser beam, electron beam, friction and ultrasound.

Laser beam welding (LBW) is non-conventional and advanced welding methods for joining similar or dissimilar materials. It possesses major advantages over other traditional welding such as deep welds, high welding speed, low heat input, high degree of automation and narrow heat affected zone [1 - 3]. Among all available laser heat sources, fiber laser gained great attractiveness due its high beam quality, light weight, high speed and good flexibility. Laser beam welding is a complex process including large number of input process parameters. The simulation of the welding process using finite element method (FEM) is able to separate the influence of each welding parameters and help to understand the various effects on temperatures profiles, distortions, and residual stresses during and after welding. LBW process is stochastic in nature. Due to this, achieving optimum process parameters just by trial-and-error method is very challenging task. Now-a-days the demand for numerical simulation is progressively increasing to attain optimum process parameters in order to reduce experimental costs [2, 3].

The thermo-mechanical analysis in welding is studied by many researchers by analytical and numerical approach. The most popular analytical model is developed by Rosenthal in 1946 in order to obtain the transient temperature histories [4].

Several researchers have pointed out that the Rosenthal model is not suitable to simulate temperature profile during fusion welding process. The temperature dependent material properties are not incorporated in his model. Goldak et al. proposed a 3-D non-axisymmetric double-ellipsoidal heat source model in order to simulate welding phenomena [5]. Frewin and Scott developed a time dependent 3-D FE model of heat flow during Nd: YAG LBW. They assumed Gaussian energy distribution of heat source in order to obtain transient temperature history in the fusion zone and HAZ. They ignored the effect of convective heat flows in weld pool [6]. A 3D FEM model was used to simulate the LBW process of AA5083 thin sheets by Spina et al. [7]. This model was very useful to predict the displacement of specimens at different welding conditions. Akbari et al. [8] also developed a 3-D model for the prediction of transient temperature profile of laser welded Ti64 alloy considering Gaussian energy distribution of laser beam. The complex physical phenomena causing the formation of keyhole mode of welding is not considered by them. The average absorptivity value of 0.34 for Ti64 alloy was considered during simulation. The thermo physical property of Ti64 alloy was also incorporated in their model. In the current study, prediction of weld bead geometry, simulation of temperature distribution of laser welded sheet at different welding conditions is carried out.

2. MATERIALS

Titanium alloy (Ti6Al4V) of Grade 5 (Ti64) is selected for the present transient thermal analysis. The melting point of Ti64 alloy is around 1690°C. It is observed from the previous research work that the temperature dependent thermo physical material properties yield better results. Hence, the thermo physical material properties (i.e. thermal conductivity, enthalpy, density, specific heat, and emissivity) of Ti64 alloy are assumed to be isotropic and homogeneous [9]. The schematic diagram of workpiece dimension and LBW experimental setup are shown in Figs. 1(a) and (b), respectively. The FE modeling procedure consists of the following steps as shown in Table. 1.

* Manas Das, Email: manasdas@iitg.ernet.in

ISBN: 978-93-80689-28-9

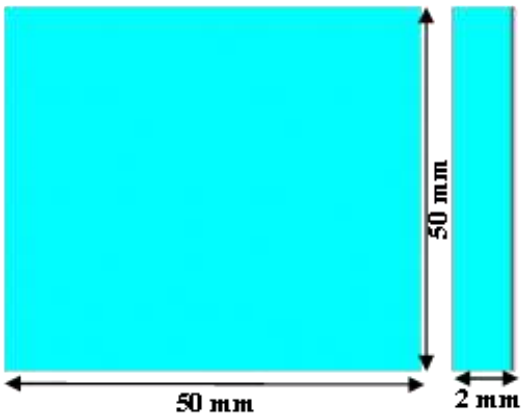

(a)

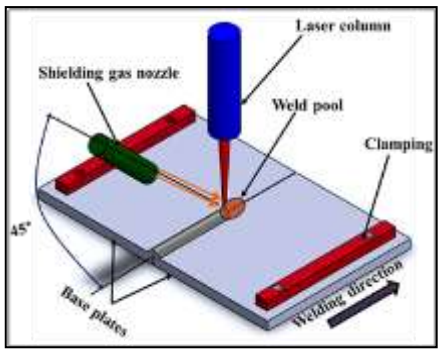

(b)

Fig. 1. Schematic diagram of (a) workpiece and its dimension and (b) LBW setup

Table 1: Finite element modeling procedure

Preprocessing	Solution	Post processing
• Element Type • Material Model • Meshing	• Define initial condition • Define load • Solve	Results

3. PREPROCESSING

The transient thermal analysis is performed in commercial FE package ANSYS® 14.5. Eight-noded quadratic 3-D solid element "SOLID70" is considered. The geometry of the workpiece is made with refined mesh near the weld line (Fig. 2 (a)) and non-uniform coarser mesh away from the weld line.

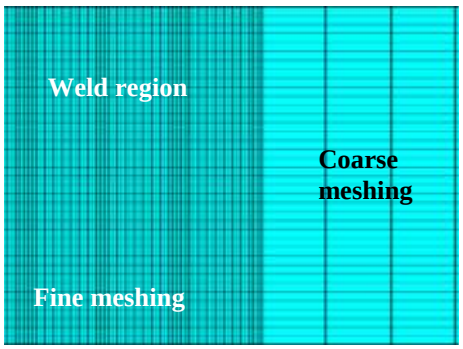

Fig. 2. Meshed workpiece along (a) weld line (fine mesh) (b) away from weld line (coarse mesh)

Convergence tests are carried out for selecting suitable number of elements particularly around the weld line and in the thickness direction. It is observed that six elements along the thickness direction give reasonable convergency with less solution time and good accuracy. The simulation is performed in two steps. In the first step, both heat flux and heat generation is applied on the surface of the workpiece. In the second step, the heat flux and heat generation is removed and the heat is dissipated from all boundaries of the workpieces by convection and radiation. The temperature dependent material properties are also considered during simulation. The effect of process parameters as show in Table 2 are studied using FE simulations on 2 mm thick Ti64 sheet.

Table 2: Laser beam welding process parameters

Welding speed (mm/min)	Power (Watt)	Beam angle (Degree)	Spot diameter (mm)
400	1200	90°	0.4
800			
1200			

4. GOVERNING EQUATION AND BOUNDARY CONDITIONS

The 3-D transient non-linear heat transfer equation for LBW process can be represented as

$$\rho c[\frac{\partial T}{\partial t}+(-v)\frac{\partial T}{\partial y}]=\frac{\partial}{\partial x}(\mathrm{K}\frac{\partial T}{\partial x})+\frac{\partial}{\partial y}(\mathrm{K}\frac{\partial T}{\partial y})+\frac{\partial}{\partial z}(\mathrm{K}\frac{\partial T}{\partial z}) \quad (1)$$
$$+Q(x,y,z)$$

where, Q(x, y, z) is volumetric heat source which varies with beam power, beam incident angle, beam exposure time, and welding speed. K, c, ρ and v are the thermal conductivity, specific heat, density of the material and the velocity of the laser heat source, respectively. The initial condition during FE simulation is given as

$$\mathrm{T}(x, y, z, 0) = \mathrm{T}_o(x, y, z) \quad (2)$$

The natural boundary condition is given as

$$K_n(\partial T/\partial n)-\mathrm{q}+\mathrm{h}(\mathrm{T}-T_o)+\sigma\varepsilon\left(T^4-T_o^4\right)=0 \quad (3)$$

A lumped heat transfer coefficient (h_{lump}) is used in the present analysis which combines both radiative and convective heat transfer phenomena [6] and it is given as

$$h_{lump}=2.4\times10^{-3}\varepsilon T^{1.61} \quad (4)$$

In Eqs. (3 & 4), K_n is thermal conductivity, q is heat flux (W/m^2 k), h is Stefan-Boltzmann constant, ε is emissivity, and T_o is ambient temperature.

4.1 Heat Source and FEM Modelling

The conical heat source consists of two parts. 1st part is plane Gaussian heat source which is distributed on the top surface of the workpiece and the 2nd part is conical shape, distributed along the thickness direction. The maximum heat intensity is

distributed on the top surface and the minimum is in the thickness direction of the workpiece. During simulation, it is considered that 25% of beam power is absorbed by the surface of the workpiece and remaining 75% is absorbed by wall of keyhole [10]. The conical Gaussian heat flux distribution is given as

$$Q(r,z) = Q_0 \exp(-\frac{3r^2}{r_0^{\,2}}) \quad (5)$$

where, Q_0 = maximum heat intensity of laser beam, r_0 = heat distribution parameter, r = radial coordinate of the interior point. Z is the coordinate of conical heat source. Assuming that the laser beam maintains a constant transverse electromagnetic mode (TEM_{00}) for conical Gaussian heat flux, the distribution can be written in terms of x and y coordinates as

$$Q(x,y) = \frac{3Q_{surf}}{\pi R^2} \exp(-3(x^2 + y^2)) \quad (6)$$

where, Q_{surf} is the plane heat source and it is considered 25% and R is the heat source radius. The heat source radius is calculated from the focal length of the focusing lens as given in Eq. (7).

$$R = \frac{2M_0^{\,2}\lambda f}{\pi D_0} \quad (7)$$

Here, $M_0^{\,2}$ is the value of beam quality, λ is the wavelength (1.08 μm) of the laser source. The value of $M_0^{\,2}$ is assumed as 1.0 for an ideal Gaussian beam. In Eq. (7), *f* is the focal length (200 mm) of the focusing lens, and D_0 is the minimum diameter of the laser beam (0.4 mm). Assuming conical shape of keyhole, the Gaussian distribution of heat flux is given as

$$Q(z) = \frac{Q_{keyhole}}{\pi r_e^2 \, H} \quad (8)$$

Where, r_e is average keyhole radius, H is thickness of sheet

5. RESULTS AND DISCUSSION

The effect of process parameters after analysing the simulation results are discussed in the following sections.

5.1. Effect of Welding Time

Figure 3 shows the transient temperature distribution on the workpiece surface at four different time steps (1 s, 2.5 s, 3.5 s and 7.5 s in Figs. 3(a), (b), (c), and (d), respectively) for 1200W welding power for 400 mm/min constant welding speed, 900 beam incident angle and 0.4 mm spot diameter. In Figs. 3 (a), (b), and (c), it is observed that the temperature profile around the laser heat source increases rapidly from ambient temperature of 27°C to peak temperature of around 5066°C for the time interval of 0 to 1 s. It is also observed that the rise in peak temperature continuously increases during time interval of 1 to 7.5 s. At this time, the peak temperature reaches up to 6835°C. The time interval between 0 to 1 s is called as initial transient stage. When the heat source reaches to the edge of the workpiece, it is observed that the value of the peak temperature is higher than the middle zone, due to the poor heat conductivity at the boundary of the workpiece. At the end of 7.5 s, the peak temperature is observed as approximately 6835°C. It is observed from Fig. 3 that the shape of the molten pool is elliptical in nature as shown by the red color. It is also noticed that the cooling rate is relatively smaller than the heating process.

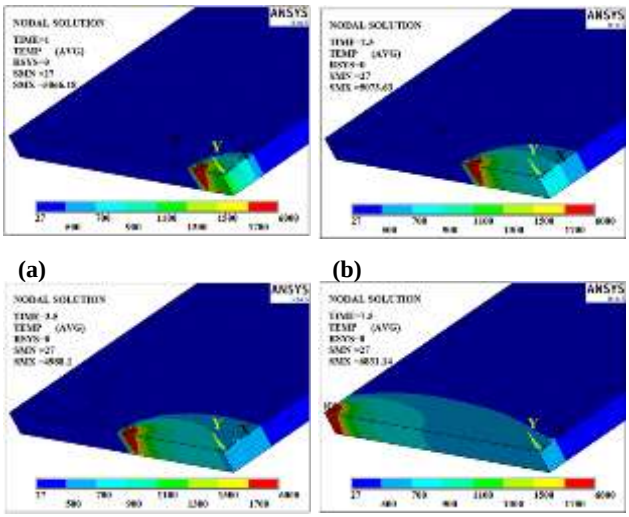

Fig. 3. Distribution of temperature (°C) at different time; (a) 1 s, (b) 2.5 s, (c) 3.5 s, and (d) 7.5s for LBW power of 1200 W and 400 mm/min welding speed

The melting point of Ti64 is around 1700°C. Hence, the width of the bead is measured as the intercept of 1700°C isotherm from temperature distribution profile along the width direction. Similarly, the depth of penetration is obtained from the temperature distribution profile along the thickness direction.

5.2. Effect of Welding Speed

It is observed from the Figs. 4 (a), (b) and (c) that the depth of penetration at constant laser beam power decreases with increasing welding speed. At 1200 W beam power and 400 mm/min welding speed, full penetration in the weld bead is obtained as shown in Fig. 4(a). Also, there is some considerable reduction in bead width at higher welding speed while doing LBW at constant welding speed. These phenomena can be explained by the absorptivity property of laser beam by the base metal. It can be attributed to the fact that at very high welding speed, the absorptivity of the laser beam by the base material is minimum due to lower interaction time with the base material which leads to lesser depth of penetration.

5.3. Distribution of Peak Temperature

Figure 5 shows the effect of laser beam power on temperature distribution at a node (a) along the weld line and (b) transverse to the weld line for 400 mm/min, 800 mm/min and 1200 mm/min welding speed and 1200 W constant beam power. It is observed that the distance between the centers of the laser beam spots and the location where the maximum temperature reaches, slightly increase as the welding speed decreases. Both the peak temperature and the temperature gradient increase as the welding speed decreases. This is due to highly concentrated laser beam power density over a very small spot area of 0.4 mm

diameter. A non-linear relationship between the peak temperature and the laser beam power is noticed as shown in Figs. 5 (a) and (b). The possible reason is due to the variation of absorption coefficient of the Ti64 alloy with temperature. The absorptivity plays an important role on the thermal field since it controls the heat input to the workpiece. Also, absorptivity is a function of surface temperature. It is also observed that the peak temperature along the weld line is very high and decreases continuously in the transverse direction away from the weld line.

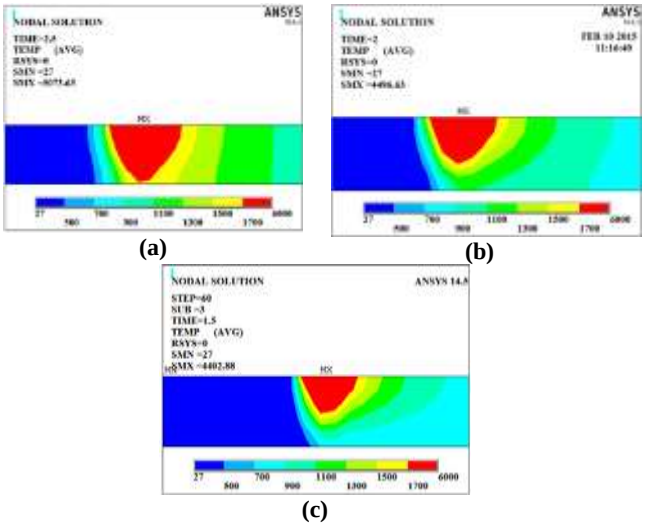

Fig. 4. Depth of penetration at different welding speeds of (a) 400, (b) 800 and (c) 1200 (mm/min) at 1200 W LBW power

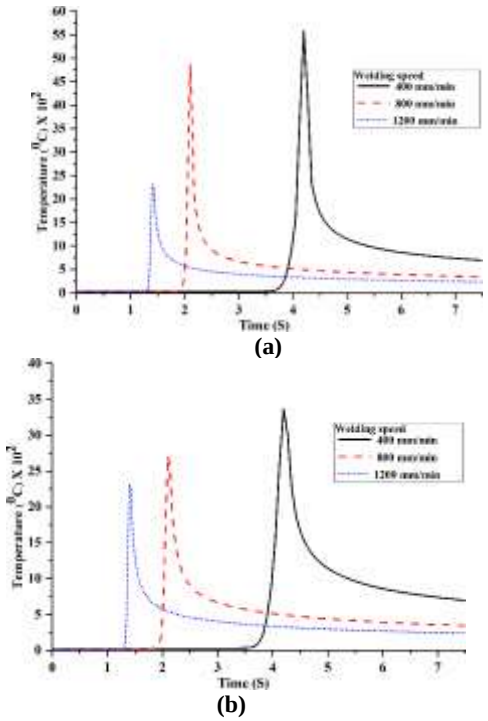

Fig. 5. Distribution of peak temperature (°C) at a node along (a) weld line and (b) transverse to the weld line at different welding speeds and 1200W constant LBW power

6. CONCLUSIONS

In this present study, a FEM simulation of laser beam welding with moving heat source on Ti64 workpiece is carried out. The following observations are found from simulation study.

- The peak temperature and depth of penetration decrease with increasing welding speed at constant beam power.
- The size of the HAZ increases as the welding speed decreases.
- The peak temperature along the weld line is very high and decreases continuously in transverse direction away from the weld line.
- A nonlinear relationship between the welding speed and peak temperature of the welded specimen are observed.
- The present model may be taken as a reference to perform the trial experiments which help in reducing cost of experiments.

References

[1] A. Costa, R. Miranda, L. Quintino, D. Yapp., Analysis of beam material interaction in welding of titanium with fiber lasers, *Materials and Manufacturing Processes*, **22** (2007) 798–803.

[2] J. Matthew and Jr. Donachie., A Technical Guide: 2nd Edition, Materials park, OH: ASM International, 2000.

[3] N. S. Shanmugam, G. Buvanashekaran, K. Sankaranarayanasamy and S. R. Kumar., A transient finite element simulation of the temperature and bead profiles of T-joint laser welds, *Materials and Design*, **31** (2010) 4528–4542.

[4] D. Rosenthal., The theory of moving source of heat and its application to metal treatment, *Transactions ASME*, **68** (1946) 849–866.

[5] J. Goldak, A. Chakravarti, M. Bibby., A new finite element model for welding heat sources, *Metallurgical Transactions*, **15**, 299-305.

[6] M. R. Frewin and D. A. Scott., Finite element model of pulsed laser welding, *Welding Research Supplement*, **78**, 15-22.

[7] R. Spina, L. Tricarico, G. Basile, T. Sibillano., Thermo mechanical modeling of laser welding of AA5083 sheets, Journal of Material Processing Technology, **191** (2007) 215–219.

[8] M. Akbari, S. Saedodin, D. Toghraie, R. Razavi, and F. Kowsari., Experimental and numerical investigation of temperature distribution and melt pool geometry during pulsed laser welding of Ti-6Al-4V alloy, *Optics and Laser Technology*, **59** (2014) 52-59.

[9] J. Yang, S. Sun, M. Brandt, W. Yan., Experimental investigation and 3D finite element prediction of the heat affected zone during laser assisted machining of Ti6Al4V alloy, *Journal of Material Processing Technology*, **210** (2010) 2215-2222.

[10] S. A. Tsirkas, P. Papanikos, T. Kermanidis., Numerical simulation of the laser welding process in butt-joint specimens, *Journal of Materials Processing Technology*, **134** (2003) 59-69.